Silicon Enolate Analogues

DOI: 10.1002/anie.201001024

Isolation of Silenolates $(R_3Si)_2Si{=}C(OLi)Ad$ with a Doubly Bonded Silicon Atom**

Roman Dobrovetsky, Lieby Zborovsky, Dennis Sheberla, Mark Botoshansky,
Dmitry Bravo-Zhivotovskii, and Yitzhak Apeloig**

Dedicated to Professor Paul von Ragué Schleyer on the occasion of his 80th birthday

Metal enolates are an important class of reactive intermediates widely employed in organic synthesis.[1] In contrast, little is known about silenolates, the silicon analogues of enolates.[2,3] Enolates exist in two tautomeric forms, the enol form and the keto form, and their reactions reflect the coexistence of these two forms.[1] The dominant structure of alkali metal enolates is the enol form both in nonsolvating media and in various solvating media such as THF, *N,N,N′,N′*-tetramethylethylenediamine, and [18]crown-6.[1] Silenolates also exist in two tautomeric forms: the keto form **a** (acyl silyl anion) and the enol form **b** (silene) [Eq. (1)], and they also show ambident reactivity.[2] The first silenolate (solvated), recently isolated and characterized by X-ray crystallography, has the keto form **a**.[3] An enol-form silenolate **b** was not yet reported. Isolation of an enol-form silenolate is challenging, because it has a Si=C π bond which is thermodynamically and kinetically less stable than a C=C bond.[4,5] In addition, enol-form silenolates can be regarded as functional silenes, which are reagents of growing importance in silicon chemistry.[6]

Here we report the synthesis, isolation, and X-ray molecular structure of the first enol-form silenolates $(t\mathrm{BuMe_2Si})_2\mathrm{Si{=}C(OLi)Ad}$ (**1**) and $(t\mathrm{Bu_2MeSi})_2\mathrm{Si{=}C(OLi)Ad}$ (**2**). We show by DFT quantum-mechanical calculations that, in contrast to organic enolates, which exist predominantly in the enol form regardless of solvation,[1] the structure of silenolates **1** and **2** is strongly dependent on the solvent.

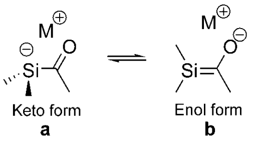

(1)

Silenolate **1** was synthesized by metal–halogen exchange between $t\mathrm{BuMe_2SiLi}$ (in excess) and bromo acyl silane $\mathrm{Br}(t\mathrm{BuMe_2Si})_2\mathrm{SiC(O)Ad}$ (**3**) in hexane at −78 °C. Upon warming to room temperature pale yellow crystals of silenolate **1** precipitated (10 % yield).[7] The major product is substitution product **4** [Eq. (2)].[7]

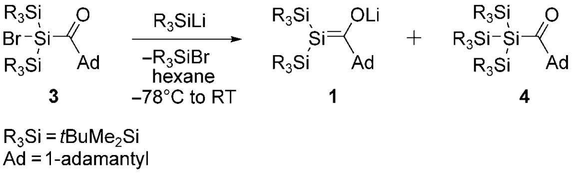

(2)

The molecular structure of **1** was determined by X-ray crystallography.[8] In the crystal, **1** is an aggregate of three $(t\mathrm{BuMe_2Si})_2\mathrm{Si{=}C(OLi)Ad}$ molecules forming a six-membered ring, in which each Li atom is coordinated to two oxygen atoms, and each oxygen atom to two Li atoms (Figure 1).

The Si=C bond length in **1** of 1.822 Å is longer than the Si=C bond (1.764 Å) in $(\mathrm{Me_3Si})_2\mathrm{Si{=}C(OSiMe_3)Ad}$ (**5**),[9] probably because of the larger substituents in **1** compared to **5**,[10] but it is significantly shorter than the Si–C bond length (1.926 Å) in acyl silyl anion $[(\mathrm{Me_3Si})_2\mathrm{SiC(O)}t\mathrm{Bu}]^-$ $\mathrm{K^+}$[18]crown-6 (**6**).[3] The essentially planar Si1 atom of **1** ($\Sigma\theta(\mathrm{Si1}) = 359.25°$) suggests sp^2 hybridization. The Si3-Si1-C1-O1 torsion angle in **1** of 9.3° is smaller than the analogous torsion angle in **5** (14.6°).[9] The O–Li bond lengths (1.858 and 1.834 Å) in **1** are in the regular range of O–Li bond lengths in enolates (1.80–1.90 Å).[11] Thus, **1** has the expected structure of an enol-form silenolate **b**, with an Si=C bond.

Aiming to obtain an enol form silenolate in higher yield, we prepared bromo acyl silane **3a**, an analogue of **3** with larger substituents ($t\mathrm{Bu_2MeSi}$ in **3a** vs. $t\mathrm{BuMe_2Si}$ in **3**). Reaction of **3a** with $t\mathrm{BuMe_2SiLi}$ at −78 °C in hexane followed by warming to room temperature gave silenolate **2** as a yellow crystalline powder in 80 % yield [Eq. (3)].[7b] The structure of **2** was determined by X-ray crystallography (Figure 2).[12]

Compound **2** is a dimer of a coaggregate of silenolate with $t\mathrm{BuMe_2SiLi}$, that is, $[(t\mathrm{Bu_2MeSi})_2\mathrm{Si{=}C(OLi)Ad}\cdot t\mathrm{BuMe_2SiLi}]_2$. The structure of the silenolate part of **2** resembles the structure of **1** (Figure 2b), although it has a different

---

[*] R. Dobrovetsky, L. Zborovsky, D. Sheberla, Dr. M. Botoshansky, Dr. D. Bravo-Zhivotovskii, Prof. Y. Apeloig
Schulich Faculty of Chemistry and the Lise Meitner-Minerva Center for Computational Quantum Chemistry, Technion-Israel Institute of Technology
Haifa 32000 (Israel)
Fax: (+972) 4-829-4601
E-mail: chrbrzh@tx.technion.ac.il
apeloig@tx.technion.ac.il

[**] This research was supported by the Israel Science Foundation, the Fund for the Promotion of Research at the Technion, and the Minerva Foundation in Munich. D.B.-Z., M.B. are grateful to the Ministry of Immigrant Absorption, State of Israel, for a Kamea scholarship. We thank I. Ben-Shir and Prof. A. Schmidt (Technion) for help with the measurement of the solid-state NMR spectrum. Ad = 1-adamantyl.

Supporting information for this article is available on the WWW under http://dx.doi.org/10.1002/anie.201001024.

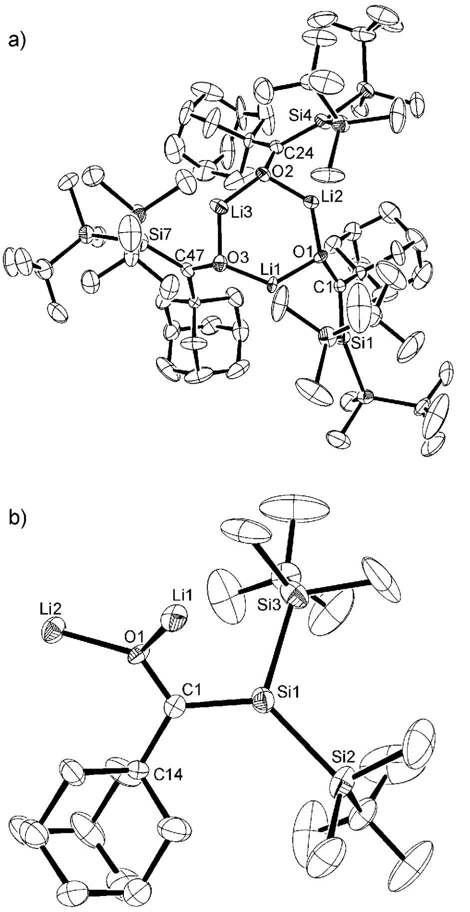

Figure 1. ORTEP of the X-ray molecular structure of **1**. Hydrogen atoms are omitted for clarity, and the thermal ellipsoids are set at 30% probability. a) Unit cell including three molecules of **1**. b) Monomeric unit of **1** (with an additional Li atom). Selected bond lengths [Å] and bond and dihedral angles [°]: Si1–C1 1.822(7), Si1–Si2 2.360(3), Si1–Si3 2.341(3), C1–O1 1.315(7), C1–C14 1.553(8), O1–Li1 1.858(12), O1–Li2 1.834(13); C1-Si1-Si2 129.9(2), C1-Si1-Si3 110.0(2), Si2-Si1-Si3 119.30(12), Si1-C1-O1 120.3(5), Si1-C1-C14 124.8(5), O1-C1-C14 115.0(6); Si3-Si1-C1-O1 9.3(2); Si2-Si1-C1-C14 −9.7(2) Si2-Si1-C1-O1 170.6(8); Li2-O1-C1-Si1 175.4(3); Li1-O1-C1-Si1 −50.2(3).

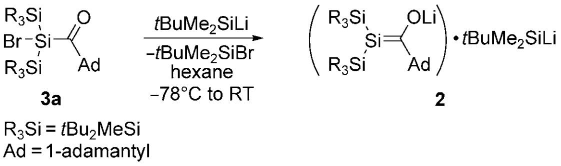

(3)

aggregation pattern. The Si=C distance is 1.811 Å and Si1 has planar geometry ($\Sigma\theta = 359.98°$). The Si3-Si1-C19-O1 torsion angle in **2** of 24.4° is significantly larger than that of **1** (9.3°) and indicates significant twisting around the Si=C bond. This is most likely due to the larger silyl substituents in **2** relative to **1** ($t\mathrm{Bu_2MeSi}$ vs. $t\mathrm{BuMe_2Si}$).

The solid-state isotropic NMR ^{29}Si chemical shift of the doubly bonded Si atom of **2** ($\delta = 8$ ppm) is shifted downfield significantly in comparison to that of the central Si atom in acyl silyl anion **6** ($\delta = -93.8$ ppm).[3] However, $\delta(^{29}\mathrm{Si})$ is shifted upfield in comparison to silene **5** ($\delta = 41.4$ ppm).[9]

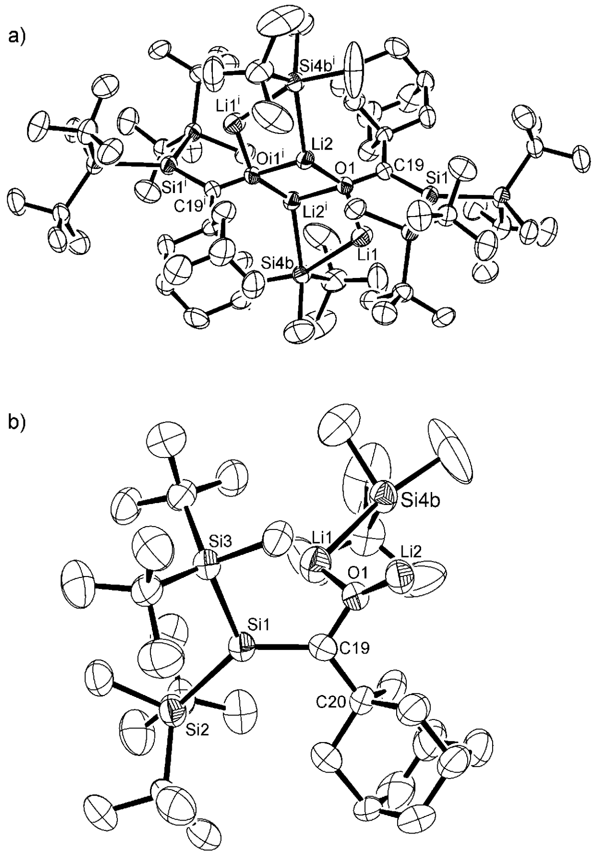

Figure 2. a) ORTEP of the X-ray molecular structure of **2**. Hydrogen atoms are omitted for clarity and the thermal ellipsoids are set at 40% probability. a) Unit cell. b) Monomeric unit of **2** aggregated with one molecule of $t\mathrm{BuMe_2SiLi}$. Selected bond lengths [Å] and bond and dihedral angles [°]: Si1–C19 1.81(2), Si1–Si2 2.418(11), Si1–Si3 2.399(13), C19–O1 1.400(2), O1–Li1 1.861(5), O1–Li2 2.028(5), O1–Li3 1.928(4); C19-Si1-Si2 129.05(8), C19-Si1-Si3 110.28(8), Si2-Si1-Si3 120.65(5), Si1-C19-O1 128.34(14); Li2-O1-C19-Si1 −136.3(4); Li1-O1-C19-Si1 103.2(4); Si3-Si1-C19-O1 24.4(3); Si2-Si1-C19-C20 23.56(4).

From the NMR and structural data we conclude that **2** is an enol-form silenolate in the solid state and most likely also in hexane solution.[13] In contrast, silenolate **6** exists predominantly in the keto form.[3] We hypothesized that the different tautomeric forms of **1** and **2** versus **6** are due to solvation. As this could not be studied experimentally[13] we relied on theory.

To better understand the effect of solvation on the structure of silenolates we carried out DFT calculations at the B3LYP 6-31G+(d) level of theory[14] for four model molecules of **1** (**1a–d**),[15] where **1a** models a monomeric unit of **1**, **1b** and **1c** model a monomeric unit of **1** aggregated with two MeOLi molecules (**1b**) or coordinated by three $\mathrm{NH_3}$ molecules (**1c**), and **1d** models a free anion of **1**.[16,17] The results of the calculations are presented in Figure 3 and Table 1.

Models **1a** and **1b** have typical silenolate structures with a planar central silicon atom ($\Sigma\theta = 360°$) and a slightly elongated Si=C bond (1.828–1.838 Å). Their HOMOs have strongly pronounced π character (Figure 3). Interestingly, the polarization in **1a** and **1b** (based on calculated Mulliken

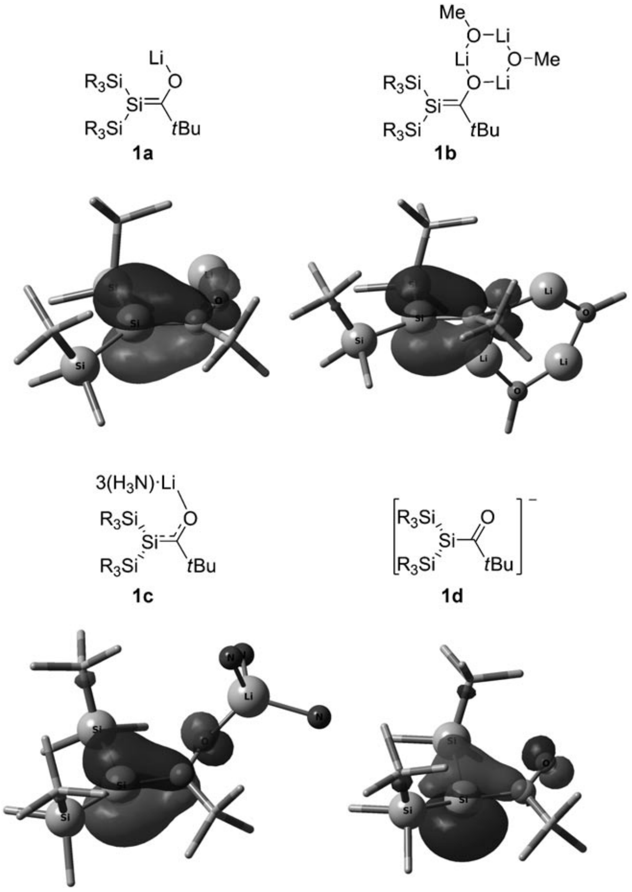

Figure 3. Calculated structures of **1a**–**d** ($R_3Si \equiv tBuMe_2Si$) and plots of their HOMOs. Hydrogen atoms are omitted for clarity. Peripheral carbon atoms are represented by sticks.

Table 1: Calculated Si=C, C=O, and O–Li bond lengths and the sum of angles around the central silicon atom in **1a**–**d**.

Parameter	**1a**	**1b**	**1c**	**1d**
r(Si=C) [Å]	1.838	1.828	1.862	1.923
r(C=O) [Å]	1.302	1.325	1.286	1.248
r(O–Li) [Å]	1.698	1.775	1.827	–
$\Sigma\theta$(Si) [°]	360	360	352	339

charges) is $Si^{\delta+}=C^{\delta-}$, although the polarity is smaller than in $H_2Si=CH_2$.[5a,18] On the other hand, **1d** has a typical structure of an acyl silyl anion with a strongly pyramidal central silicon atom ($\Sigma\theta = 339°$) and a long Si–C distance (1.922 Å) typical of a C–Si single bond (e.g., 1.94 Å in ($tBuMe_2Si)_3SiC(=O)Ad$ (**4**)[19]), and its HOMO, which is mainly concentrated on the central silicon atom, is characteristic of a silyl anion. Models **1b** and **1c** have intermediate geometries between **1a** and **1d**. Model **1c**, with stronger complexation of the lithium atom (by three NH_3 molecules), has a somewhat longer Si–C bond length (1.862 Å) and a slightly pyramidal central Si atom ($\Sigma\theta = 352°$) compared to **1b** (r(Si=C) = 1.828 Å, $\Sigma\theta = 360°$). The HOMO of **1c**, similarly to **1a** and **1b**, has pronounced π character (Figure 3). The moderate elongation of the Si–C bond and the small distortion from planarity around Si in **1c** compared to **1a** indicate that **1c** has an intermediate structure along the enol–keto coordinate. Thus, the calculations show that as the Li atom is better solvated (e.g., in **1c**) and the Li–O distance increases **1** adopts a more pronounced acyl-silane character.[20] This is supported by the fact that **6** with a strongly solvated K^+ ion adopts the keto form.[3]

To further support the relation between solvation and structure, we carried out additional B3LYP 6-31G+(d) calculations for **1a** and the analogous carbon enolate $(Me_3Si)_2C=C(OLi)tBu$ (**7**), in which the Li–O distance was elongated in five equal steps (0.45 Å in **1a** and 0.5 Å in **7**) from the optimized distances to 3.95 Å in **1a** and 4.16 Å in **7**. At each Li–O distance full optimization of the geometry was carried out, except for the C-O-Li angle, which was kept at 140° in **1a** and 147° in **7**. We find (Figure 4a) that, when the Li–O distance is short, the Si–C bond length is also short (1.838 Å), and the central silicon atom is planar ($\Sigma\theta = 359.9°$), that is, **1** adopts an enol-form silenolate geometry. Upon elongating the Li–O distance the structure of **1** continuously shifts towards that of the keto form (**1d**), with a longer Si–C bond (1.93 Å, Figure 4a) and a pyramidal central silicon atom ($\Sigma\theta = 336°$, Figure 4b). In contrast, the carbon enolate **7** is only slightly affected by elongation of the Li–O distance (Figure 4), and this suggests that its structure is not significantly altered by solvation.

Steric repulsion also plays a role in determining the position of the structure along the enol–keto coordinate.

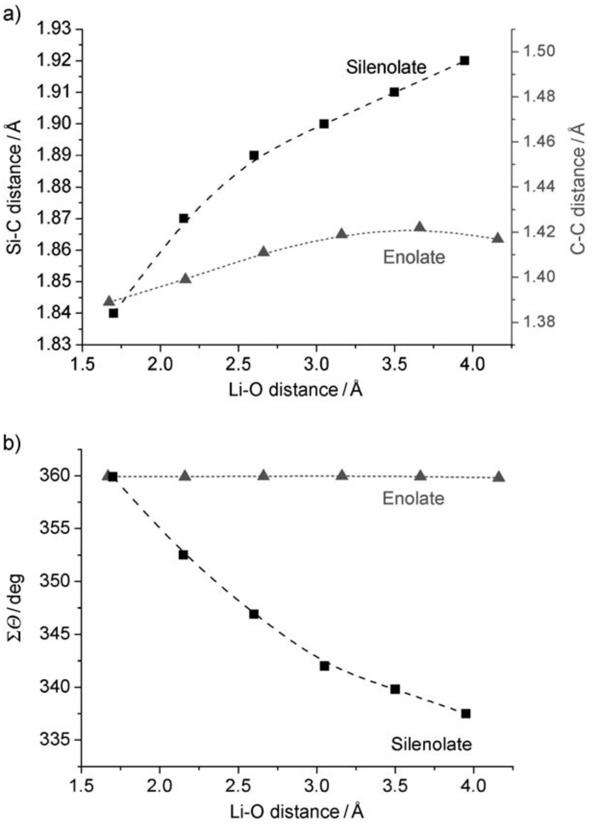

Figure 4. a) Calculated Si–C bond lengths for **1a** and C–C bond lengths for **7** versus Li–O distance. b) Calculated sum of bond angles around the α-E atom (for silenolate **1a** and enolate **7** versus Li–O distance.

Calculations on [$(Me_3Si)_2Si{=}C(OLi)t$Bu]·LiOMe (**6a**) show that the central silicon atom is pyramidal ($\Sigma\theta = 336°$) in contrast to **1b** with larger tBuMe$_2$Si substituents, which is planar ($\Sigma\theta = 360°$). The Si=C bond length in **6a** (1.842 Å) is also longer than that in in **1b** (1.828 Å).[19] Thus, large substituents shift the structure towards the enol-form silenolate.

In conclusion, we have synthesized, isolated, and characterized by X-ray crystallography the first two enol-form silenolates **1** and **2**. Density functional calculations showed that, in contrast to organic enolates, which predominantly adopt the enol form regardless of solvent, the structure of silenolates strongly depends on the solvent. In nonsolvating media the enol form of the silenolate dominates, but effective solvation of the cation, for example, by crown ethers,[3] strongly favors the keto form. Further studies on the keto–enol equilibrium of silenolates are underway.

Received: February 18, 2010

Keywords: density functional calculations · enols · silenes · silicon · tautomerism

---

[1] For reviews, see: a) D. Stolz, U. Kazmaier in *The Chemistry of Metal Enolates*, Part 1 (Eds.: Z. Rappoport, J. Zabicky), Wiley, Hoboken, **2009**, pp. 355–411; b) D. Seebach, *Angew. Chem.* **1988**, *100*, 1685–1715; *Angew. Chem. Int. Ed. Engl.* **1988**, *27*, 1624–1654; c) P. Veya, C. Floriani, A. Chiessi-Villa, C. Rizzoli, *Organometallics* **1994**, *13*, 214–223.

[2] For example a) J. Ohshita, S. Masaoka, Y. Masaoka, H. Hasebe, M. Ishikawa, *Organometallics* **1996**, *15*, 3136–3146; b) J. Ohshita, S. Masaoka, M. Ishikawa, *Organometallics* **1996**, *15*, 2198–2200; c) J. Ohshita, S. Masaoka, Y. Morimoto, *Organometallics* **1997**, *16*, 910–917; d) J. Ohshita, S. Masaoka, Y. Morimoto, M. Sano, *Organometallics* **1997**, *16*, 1123–1129; e) J. Ohshita, H. Sakurai, Y. Tokunaga, A. Kunai, *Organometallics* **1999**, *18*, 4545–4551; f) J. Ohshita, Y. Tokunaga, H. Sakurai, A. Kunai, *J. Am. Chem. Soc.* **1999**, *121*, 6080–6081; g) J. Ohshita, H. Sakurai, S. Masaoka, M. Tamai, A. Kunai, M. Ishikawa, *J. Organomet. Chem.* **2001**, *633*, 131–136.

[3] T. Guliashvili, I. El-Sayed, A. Fischer, H. Ottosson, *Angew. Chem.* **2003**, *115*, 1678–1680; *Angew. Chem. Int. Ed.* **2003**, *42*, 1640–1642.

[4] H. Ottosson, A. M. Eklof, *Coord. Chem. Rev.* **2008**, *252*, 1287–1314.

[5] a) Y. Apeloig, M. Karni, *J. Am. Chem. Soc.* **1984**, *106*, 6676–6682; b) Y. Apeloig in *The Chemistry of Organic Silicon Compounds*, Part 1 (Eds.: S. Patai, Z. Rappoport), Wiley, New York, **1989**, p. 57–225.

[6] D. Scheschkewitz, *Chem. Eur. J.* **2009**, *15*, 2476–2485.

[7] a) The low yield of **1** and the poor reproducibility of its synthesis prevented its systematic spectroscopic characterization; b) For synthetic procedure, see Supporting Information.

[8] Crystallographic data for **1**: $C_{69}H_{135}Li_3O_3Si_9$, $M_r = 1286.40$, monoclinic, space group $P2_1/c$, $a = 20.603(4)$, $b = 24.993(5)$, $c = 16.483(3)$ Å, $\beta = 105.61(3)°$, $V = 8175(3)$ Å^3, $Z = 4$, Nonius Kappa CCD, Mo$_{K\alpha}$ radiation (0.71073 Å), 240 K, $2\Theta_{max} = 25°$, $R = 0.0802$ [$I > 2\sigma(I)$], $wR2 = 0.1401$ [$I > 2\sigma(I)$], $Rw = 0.1860$ (all data), GOF = 0.821. CCDC 760801 contains the supplementary crystallographic data for this paper. These data can be obtained free of charge from The Cambridge Crystallographic Data Centre via www.ccdc.cam.ac.uk/data_request/cif.

[9] a) A. G. Brook, S. C. Nyburg, F. Abdesaken, B. Gutekunst, G. Gutekunst, R. Krishna, M. R. Kallury, Y. C. Poon, Y. M. Chang, W. N. Winnie, *J. Am. Chem. Soc.* **1982**, *104*, 5667–5672; b) S. C. Nyburg, A. G. Brook, F. Abdesaken, G. Guteknust, W. Wong-Ng, *Acta Crystallogr.* **1985**, *41*, 1632–1635.

[10] Based on B3LYP/6-31(d) calculations the r(Si=C) in (tBuMe$_2$Si)$_2$Si=C(OSiMe$_3$)Ad (1.801 Å) is 0.015 Å longer than the calculated value of **5** (1.786 Å).

[11] P. G. Williard, G. B. Carpenter, *J. Am. Chem. Soc.* **1985**, *107*, 3345–3346.

[12] Crystallographic data for **2**: $C_{38}H_{79}Li_2OSi_4$, $M_r = 678.25$, triclinic, space group $P\bar{1}$, $a = 12.017(2)$, $b = 13.747(3)$, $c = 13.927(3)$ Å, $\beta = 79.69(2)°$, $V = 2197.1(8)$ Å^3, $Z = 2$, Nonius Kappa CCD, Mo$_{K\alpha}$ radiation (0.71073 Å), 240 K, $2\Theta_{max} = 25°$, $R = 0.0872$ [$I > 2\sigma(I)$], $wR2 = 0.2122$ [$I > 2\sigma(I)$], $Rw = 0.1937$ (all data), GOF = 0.986. CCDC 760802 contains the supplementary crystallographic data for this paper. These data can be obtained free of charge from The Cambridge Crystallographic Data Centre via www.ccdc.cam.ac.uk/data_request/cif.

[13] Compound **2** was crystallized from hexane; however, after precipitation **2** is not soluble in hexane or benzene, and in THF it undergoes chemical transformation; therefore, its solution NMR spectra could not be measured.

[14] The Gaussian 03 series of programs was used. All molecules were fully optimized at the B3LYP 6-31G+(d) level of theory and all structures were confirmed as local minima by calculating second order derivatives. For full details see Supporting Information.

[15] Partially reported by us at the 15th International Symposium on Organosilicon Chemistry (ISOS-XV), Jeju, South Korea, June 1–6, **2008**, Book of abstracts, 162.

[16] Calculations for simple silenolates were reported,[2b,3,17] but they did not consider the effect of substituents.

[17] A. M. Elkof, H. Ottosson, *Tetrahedron* **2009**, *65*, 5521–5526.

[18] H. Ottosson, *Chem. Eur. J.* **2003**, *9*, 4144–4155.

[19] D. Bravo-Zhivotovskii, R. Dobrovetsky, D. Nemirovsky, V. Molev, M. Bendikov, G. Molev, M. Botashansky, Y. Apeloig, *Angew. Chem.* **2008**, *120*, 4415–4417; *Angew. Chem. Int. Ed.* **2008**, *47*, 4343–4345.

[20] In all calculated molecules a minimum in which Li is bonded to Si was not found. We are well aware that the B3LYP functional tends to overestimate the degree of pyramidalization at silicon (I. Bejan, D. Güclü, S. Inoue, M. Ichinohe, A. Sekiguchi, D. Scheschkewitz, *Angew. Chem.* **2007**, *119*, 3413–3416; *Angew. Chem. Int. Ed.* **2007**, *46*, 3349–3352). However, the calculated geometries of the silenolates are in good agreement with the experimental geometries of **1**, **2**, and **6**.